

starting material, and the formation of a bicyclic phosphazene cannot be detected. This result suggests that the formation of the intramolecular P-N-P bridge and the replacement of the chlorine at the junction P atom(s) [P(2), P(6)] by the attacking nucleophile are synchronous. Further work to extend the scope of the synthetic strategy outlined above for the preparation of bicyclic phosphazenes containing a variety of substituents is in progress.

Acknowledgment. The authors thank Defence Research Laboratory, Gwalior, India, for elemental analyses and S. Raju of the Molecular Biophysics Unit of this Institute for recording the ^{31}P NMR spectra.

Registry No. III, 24587-11-9; IV, 60998-10-9; V, 94732-76-0; VI, 94732-77-1; VII, 94732-78-2; VIII, 94732-79-3; $\text{N}_4\text{P}_4(\text{NMe}_2)_5\text{-}(\text{NHEt})(\text{NEt})$, 58752-23-1; $\text{N}_4\text{P}_4\text{Cl}_2(\text{NMe}_2)_2(\text{NHEt})(\text{NEt})(\text{NC}_4\text{H}_9\text{O})$, 94732-80-6; $\text{N}_4\text{P}_4\text{Cl}_2(\text{NMe}_2)_2(\text{NHEt})(\text{NEt})(\text{NH-}i\text{-Pr})$, 94732-81-7; EtNH_2 , 75-04-7; Me_2NH , 124-40-3; morpholine, 110-91-8; isopropylamine, 75-31-0.

Department of Inorganic and Physical
Chemistry
Indian Institute of Science
Bangalore 560 012, India

P. Y. Narayanaswamy
K. S. Dhathathreyan
S. S. Krishnamurthy*

Received September 5, 1984

Articles

Contribution from the Department of Chemistry,
University of British Columbia, Vancouver, B.C., Canada V6T 1Y6

Synthesis and Stereochemistry of Reactive Mono(amido phosphine) Derivatives of Zirconium(IV) and Hafnium(IV). X-ray Crystal Structures of *fac*- $\text{HfCl}_3[\text{N}(\text{SiMe}_2\text{CH}_2\text{PMe}_2)_2]$ and *mer*- $\text{ZrCl}_3[\text{N}(\text{SiMe}_2\text{CH}_2\text{P}(\text{CHMe}_2)_2)_2]$

MICHAEL D. FRYZUK,*¹ ALAN CARTER, and AXEL WESTERHAUS

Received June 4, 1984

The tetrahalides of Zr and Hf react with 1 equiv of the potentially tridentate hybrid ligand, $\text{LiN}(\text{SiMe}_2\text{CH}_2\text{PR}_2)_2$ ($\text{R} = \text{Me}$, *i*-Pr, *t*-Bu), to generate the corresponding mono(ligand) complexes $\text{MCl}_3[\text{N}(\text{SiMe}_2\text{CH}_2\text{PR}_2)_2]$ ($\text{M} = \text{Zr}$, Hf). The stereochemistries of $\text{HfCl}_3[\text{N}(\text{SiMe}_2\text{CH}_2\text{PMe}_2)_2]$ and $\text{ZrCl}_3[\text{N}(\text{SiMe}_2\text{CH}_2\text{P}(\text{CHMe}_2)_2)_2]$ are described. In the case of the hafnium derivative, two different solid-state structures are observed: (a) monoclinic, space group $P2_1/n$, $a = 9.6894$ (10) Å, $b = 16.5806$ (6) Å, $c = 13.6613$ (13) Å, $\alpha = \gamma = 90^\circ$, $\beta = 92.214$ (4) $^\circ$, $Z = 4$, $R = 0.024$, $R_w = 0.030$; (b) orthorhombic, space group $Pbcn$, $a = 13.3517$ (8) Å, $b = 20.595$ (2) Å, $c = 15.9398$ (7) Å, $\alpha = \beta = \gamma = 90^\circ$, $Z = 8$, $R = 0.043$, $R_w = 0.046$. In both the monoclinic and orthorhombic modifications, the ligand in $\text{HfCl}_3[\text{N}(\text{SiMe}_2\text{CH}_2\text{PMe}_2)_2]$ is bound in a tridentate facial mode that deviates from a pure octahedral geometry. The zirconium complex, $\text{ZrCl}_3[\text{N}(\text{SiMe}_2\text{CH}_2\text{P}(\text{CHMe}_2)_2)_2]$, crystallizes in an orthorhombic crystal system, space group $P2_12_12_1$, $a = 9.0512$ (5) Å, $b = 17.0325$ (11) Å, $c = 17.2332$ (6) Å, $\alpha = \beta = \gamma = 90^\circ$, $Z = 4$, $R = 0.029$, $R_w = 0.034$; this solid-state structure shows a distorted octahedral geometry, wherein the tridentate ligand is bound in a meridional fashion. In solution the ligand adopts a meridional binding mode for all the $\text{MCl}_3[\text{N}(\text{SiMe}_2\text{CH}_2\text{PR}_2)_2]$ derivatives. The origins of the solid-state and solution structures are discussed.

Introduction

The stereochemistry of the group 4 transition-metal coordination compounds that do not contain cyclopentadienyl type ligands is relatively unexplored.² This is no doubt due to a number of factors including the absence of a particular stereochemical preference for early-transition-metal complexes,³ their propensity for high coordination numbers, and their high lability⁴ especially with neutral ligands. One potential inroad to overcoming some of these problems is through the incorporation of a multidentate ligand both to control stereochemistry and to reduce the lability of certain donors. We have recently reported^{5,6} the synthesis of a chelating ligand containing both "hard" and "soft" donors and its incorporation onto Zr(IV) and Hf(IV). We report here the synthesis of reactive mono(ligand) derivatives of the general formula $\text{MCl}_3[\text{N}(\text{SiMe}_2\text{CH}_2\text{PR}_2)_2]$ ($\text{M} = \text{Zr}$, Hf; $\text{R} = \text{Me}$, *i*-Pr, *t*-Bu) and their stereochemistries both in the solid state and in solution.

Experimental Section

General Information. All manipulations were performed under pre-purified nitrogen in a Vacuum Atmospheres HE-553-2 glovebox equipped with a MO-40-2H purification system or in standard Schlenk-type glassware. ZrCl_4 (Aldrich) and HfCl_4 (Alfa) were sublimed prior to use.

The secondary phosphines, HPMe_2 ,⁷ $\text{HP}(i\text{-Pr})_2$,⁸ and $\text{HP}(t\text{-Bu})_2$,⁹ were prepared according to literature procedures. Solvents were dried, distilled, and degassed by standard procedures. Melting points were determined on a Mel-Temp apparatus in sealed capillaries under nitrogen and are uncorrected. Carbon, hydrogen, nitrogen, and halogen analyses were performed by P. Borda of this department. ^1H NMR spectra were performed on one of the following instruments, depending on the complexity of the particular spectrum: Varian EM-360L, Bruker WP-80, Varian XL-100, Bruker WH-400. $^{31}\text{P}\{^1\text{H}\}$ NMR spectra were run at 32.442 MHz on the WP-80 or at 40.5 MHz on the XL-100; all ^{31}P chemical shifts are referenced to external $\text{P}(\text{OMe})_3$ set at +141.0 ppm relative to 85% H_3PO_4 . Solution $^{13}\text{C}\{^1\text{H}\}$ NMR spectra were run at 20.11 MHz on the WP-80. Infrared spectra were run on a Nicolet 5D-X instrument. Deuterated benzene (C_6D_6) and deuterated toluene (C_7D_8) were obtained from Aldrich, dried over activated 4-Å molecular sieves, and vacuum transferred prior to use. Deuterated methylene chloride (CD_2Cl_2) was dried by refluxing over CaH_2 for a few days and vacuum transferred before use.

$\text{LiN}(\text{SiMe}_2\text{CH}_2\text{PMe}_2)_2$. Dimethylphosphine (10 g, 0.161 mol) was vacuum transferred to a cooled (-80°C) flask containing a solution of *n*-butyllithium (120 mL, 1.6 M in hexanes, 0.192 mol) in hexanes (100 mL). The reaction mixture was slowly warmed to room temperature and stirred for 12 h. The resulting white precipitate was filtered off under nitrogen, washed with plenty of hexanes to remove the excess *n*-BuLi, and dried under vacuum. All of the lithium dimethylphosphide was dissolved in tetrahydrofuran (THF) (100 mL) and the resultant mixture cooled to -4°C , whereupon neat 1,3-bis(chloromethyl)tetramethyldisilazane, $\text{HN}(\text{SiMe}_2\text{CH}_2\text{Cl})_2$ ¹⁰ (11.7 g, 0.053 mol), was added dropwise with

- (1) Fellow of the Alfred P. Sloan Foundation, 1984-1986.
- (2) Kepert, D. L. "The Early Transition Elements"; Academic Press: New York, 1972; pp 1-23, 61-141.
- (3) Cotton, F. A.; Wilkinson, G. "Advanced Inorganic Chemistry", 4th ed.; Wiley: Toronto, 1980; p 826.
- (4) MacDermott, T. E. *Coord. Chem. Rev.* 1973, 11, 1-20.
- (5) Fryzuk, M. D.; Williams, H. D.; Rettig, S. J. *Inorg. Chem.* 1983, 22, 863-868.
- (6) Fryzuk, M. D.; Williams, H. D. *Organometallics* 1983, 2, 162-164.

- (7) Parshall, G. W. *Inorg. Synth.* 1968, 11, 157-159.
- (8) Issleib, K.; Krech, F. J. *Organomet. Chem.* 1968, 13, 283-289.
- (9) Hoffmann, H.; Schellenbeck, P. *Chem. Ber.* 1966, 99, 1134-1141.

stirring; the end point is indicated by the initial yellow solution fading to colorless. After the mixture was warmed to room temperature, the volatiles were removed under vacuum and the pasty white residue was extracted with hexanes (3 × 75 mL) and filtered through a medium frit. The filtrate was evaporated down to a colorless oil that was sublimed at 100 °C (10⁻³ mm) to give white crystals: yield 11.4 g (75%); mp 80–81 °C. Anal. Calcd for C₁₀H₂₈LiNP₂Si₂: C, 41.79; H, 9.82; N, 4.87. Found: C, 42.00; H, 9.90; N, 4.66. ¹H NMR (C₆D₆, ppm): PCH₃ 0.72 (s), PCH₂Si 0.42 (br d), SiCH₃ 0.33 (s). ³¹P{¹H} NMR (C₆D₆, ppm): -56.2 (s). A minor side product (<10%) that can sometimes be observed is the amine HN(SiMe₂CH₂PM₂)₂; isolation can be achieved by distillation of the crude product in a molecular still before sublimation; bp 80–90 °C (10⁻³ mm). ¹H NMR (C₆D₆, ppm): PCH₃ 0.93 (d, ²J_P = 2.0 Hz), PCH₂Si 0.51 (d, ²J_P = 2.0 Hz), SiCH₃ 0.18 (d, ⁴J_P = 1.0 Hz). ³¹P{¹H} NMR (C₆D₆, ppm): -55.7 (s). Anal. Calcd for C₁₀H₂₈NP₂Si₂: C, 42.67; H, 10.38; N, 4.97. Found: C, 42.67; H, 10.44; N, 4.93.

LiN(SiMe₂CH₂P(*i*-Pr))₂. *n*-Butyllithium (62.5 mL, 1.6 M in hexanes, 0.10 mol) was added all at once to diisopropylphosphine (10 g, 0.085 mol) in hexanes (100 mL) at room temperature and the mixture stirred for 4 days. The copious white precipitate of LiP(*i*-Pr)₂ was filtered, washed with plenty of hexanes to remove the excess *n*-BuLi, and dried under vacuum. All of the lithium diisopropylphosphide was dissolved in THF (100 mL) and the resultant mixture cooled to -4 °C whereupon neat HN(SiMe₂CH₂Cl)₂ (6.3 g, 0.028 mol) was added dropwise. After the mixture was warmed to room temperature, the volatiles were removed under vacuum; the residue was extracted with hexanes (3 × 50 mL), filtered through a medium frit, and reduced to approximately one-third volume. Cooling to -30 °C for 24 h gave large white crystals, yield 5.6 g (50.1%). ¹H NMR (C₆D₆, ppm): PCH(CH₃)₂ 1.71 (m), PCH(CH₃)₂ 1.09 (quin, ³J_P = 6.0 Hz), PCH₂Si 0.69 (d, ²J_P = 6.0 Hz), SiCH₃ 0.39 (s). ³¹P{¹H} NMR (C₆D₆, ppm): -3.28 (s). Anal. Calcd for C₁₈H₄₄NLiP₂Si₂: C, 54.10; H, 11.10; N, 3.51. Found: C, 53.70; H, 11.20; N, 3.52.

LiN(SiMe₂CH₂P(*t*-Bu))₂. To a cold (-78 °C) toluene slurry (~30 mL) of LiP(*t*-Bu)₂ (7.0 g, 0.046 mol), prepared by stirring *n*-BuLi and HP(*t*-Bu)₂ for 6 days, was added THF (100 mL), and the resulting yellow solution was allowed to warm to -15 °C slowly; to this solution was added neat HN(SiMe₂CH₂Cl)₂ (3.53 g, 0.0153 mol) dropwise. The workup was identical with that described for the isopropyl derivative; recrystallization from hexanes (-30 °C) afforded a 60% yield of sticky white crystals. ¹H NMR (C₆D₆, ppm): PC(CH₃)₃ 1.10 (br d, ³J_P = 12 Hz), PCH₂Si 0.56 (d, ²J_P = 8.2 Hz), SiCH₃ 0.34 (d, ⁴J_P = ~1 Hz). ³¹P{¹H} NMR (C₆D₆, ppm): 18.2 (s). So far, we have been unable to obtain this material in analytically pure form.

HfCl₃[N(SiMe₂CH₂PM₂)₂]. To a rapidly stirred slurry of HfCl₄ (7.80 g, 24.4 mmol) in toluene (2000 mL) was added a solution of LiN(SiMe₂CH₂PM₂)₂ (7.0 g, 24.4 mmol) in toluene (10 mL) dropwise over a period of 10 min, and the resulting mixture was stirred for 5 days at room temperature. After filtration through Celite, the clear, colorless solution was evaporated down until crystallization began. Addition of an equal volume of hexanes and cooling to -30 °C gave colorless prisms, yield 12.1 g (88%). ¹H NMR (C₆D₆, ppm): PCH₃ 0.96 (filled-in d, ²J_P + ⁴J_P = 7.5 Hz), PCH₂Si 0.83 (filled-in d, ²J_P + ⁴J_P = 11.5 Hz), SiCH₃ 0.22 (s). ³¹P{¹H} NMR (C₆D₆, ppm): -16.4 (s). ¹³C{¹H} NMR (CD₂Cl₂, ppm, -70 °C): PCH₂Si 15.90 (virtual t, ¹J_P + ³J_P = 4.9 Hz), PCH₃ 11.54 (virtual t, ¹J_P + ³J_P = 17.1 Hz), SiCH₃ 4.41 (s). Mol wt (Signer, isothermal distillation; CH₂Cl₂): 575 ± 20; calcd 565.30. Anal. Calcd for C₁₀H₂₈Cl₃HfNSi₂P₂: C, 21.25; H, 4.98; N, 2.47; Cl, 18.81. Found: C, 21.56; H, 5.03; N, 2.34; Cl, 18.77. IR (CsI, cm⁻¹): Hf-N 397; Hf-Cl 311, 286.

ZrCl₃[N(SiMe₂CH₂PM₂)₂]. The identical conditions described above for the analogous hafnium derivative were used; yield 90%. ¹H NMR (C₆D₆, ppm): PCH₃ 0.95 (filled-in d, ²J_P + ⁴J_P = 7.8 Hz), PCH₂Si 0.84 (filled-in d, ²J_P + ⁴J_P = 11.2 Hz), SiCH₃ 0.21 (s). ³¹P{¹H} NMR (C₆D₆, ppm): -16.1 (s). Anal. Calcd for C₁₀H₂₈Cl₃ZrNSi₂P₂: C, 25.12; H, 5.90; N, 2.92; Cl, 22.25. Found: C, 25.43; H, 6.00; N, 2.80; Cl, 22.00. IR (CsI, cm⁻¹): Zr-N 407, 387; Zr-Cl 349, 332, 324, 310, 295, 282.

HfCl₃[N(SiMe₂CH₂P(*i*-Pr))₂]. A solution of LiN(SiMe₂CH₂P(*i*-Pr))₂ (1.25 g, 3.13 mmol) in toluene (20 mL) was added dropwise to a rapidly stirred slurry of HfCl₄ (1.0 g, 3.13 mmol) in toluene (100 mL). The reaction mixture was stirred at room temperature for 18 h and filtered through Celite and the toluene removed under vacuum. The residue was recrystallized from minimum toluene by the addition of hexanes to give colorless prisms, yield 1.93 g (91.2%). ¹H NMR (C₆D₆, ppm): PCH(CH₃)₂ 2.0 (br m), PCH(CH₃)₂ 1.06 (quin, ³J_P = ³J_{CH} = 6.0 Hz), PCH₂Si 0.99 (t, ²J_{app} = 5.0 Hz), SiCH₃ 0.36 (s). ³¹P{¹H} NMR (C₆D₆, ppm): 20.6 (s). Anal. Calcd for C₁₈H₄₄Cl₃HfNP₂Si₂: C, 31.91;

H, 6.54; N, 2.06; Cl, 15.69. Found: C, 32.25; H, 6.71; N, 2.13; Cl, 15.85. IR (CsI, cm⁻¹): Hf-N 397; Hf-Cl 312, 297.

ZrCl₃[N(SiMe₂CH₂P(*i*-Pr))₂]. The identical conditions described above for the analogous hafnium derivative were used; yield 91%. ¹H NMR (C₆D₆, ppm): PCH(CH₃)₂ 1.95 (br m), PCH(CH₃)₂ 1.10 (quin, ³J_P = ³J_{CH} = 9.0 Hz), PCH₂Si obscured; SiCH₃ 0.42 (s). ³¹P{¹H} NMR (C₆D₆, ppm): 15.1 (s). Anal. Calcd for C₁₈H₄₄Cl₃ZrNP₂Si₂: C, 36.63; H, 7.51; N, 2.37; Cl, 18.02. Found: C, 36.97; H, 7.58; N, 2.44; Cl, 17.77. IR (CsI, cm⁻¹): Zr-N 401; Zr-Cl 322, 309.

HfCl₃[N(SiMe₂CH₂P(*t*-Bu))₂]. A solution of LiN(SiMe₂CH₂P(*t*-Bu))₂ (4.0 g, 8.79 mmol) in toluene (30 mL) was added dropwise to a slurry of HfCl₄ (2.81 g, 8.79 mmol) in toluene (150 mL). The reaction mixture was stirred at room temperature for 1 day and filtered through Celite and the toluene removed under vacuum. The residue was recrystallized from minimum toluene by the addition of hexanes and cooling to -30 °C to give long, white needles, yield 5.24 g (81.4%). ¹H NMR (C₆D₆, ppm): PC(CH₃)₃ 1.30 (filled-in d, ²J_P + ⁵J_P = 13.2 Hz), PCH₂Si 1.07 (filled-in d, ²J_P + ⁴J_P = 10.5 Hz), SiCH₃ 0.47 (s). ³¹P{¹H} NMR (C₆D₆, ppm): 38.5 (s). Anal. Calcd for C₂₂H₅₂Cl₃HfNP₂Si₂: C, 36.02; H, 7.14; N, 1.91; Cl, 14.50. Found: C, 35.86; H, 7.19; N, 1.85; Cl, 14.30. Mp: 249–251 °C. IR (CsI, cm⁻¹): Hf-N 398; Hf-Cl 296.

ZrCl₃[N(SiMe₂CH₂P(*t*-Bu))₂]. The identical conditions described above for the analogous hafnium derivative were used; yield 85%. ¹H NMR (C₆D₆, ppm): PC(CH₃)₃ 1.26 (filled-in d, ²J_P + ⁵J_P = 13.5 Hz), PCH₂Si 1.08 (filled-in d, ²J_P + ⁴J_P = 10.1 Hz), SiCH₃ 0.50 (s). ³¹P{¹H} NMR (C₆D₆, ppm): 33.85 (s). Anal. Calcd for C₂₂H₅₂Cl₃ZrNP₂Si₂: C, 40.88; H, 8.11; N, 2.17; Cl, 16.45. Found: C, 41.16; H, 8.30; N, 2.13; Cl, 16.21. Mp: 234–236 °C. IR (CsI, cm⁻¹): Zr-N 399; Zr-Cl 325, 304.

X-ray Crystallographic Analyses of HfCl₃[N(SiMe₂CH₂PM₂)₂] and ZrCl₃[N(SiMe₂CH₂P(*i*-Pr))₂]. Two crystalline forms¹¹ of the Hf complex were isolated, one monoclinic and the other orthorhombic. Crystallographic data appear in Table I. Final unit cell parameters were obtained by least squares on 2sin θ/λ values for 25 reflections with 2θ = 35–45°. The intensities of three check reflections were monitored every hour throughout the data collections and in each case showed only small random fluctuations. The data were processed¹² and absorption corrections applied by using the Gaussian integration method.^{13,14}

All three structures were solved by conventional heavy-atom methods, the metal, P, Si, and Cl positions being determined from the Patterson functions and those of the remaining non-hydrogen atoms from subsequent difference syntheses. In the final cycles of full-matrix least-squares refinement the non-hydrogen atoms were refined with anisotropic thermal parameters, hydrogen atoms being included as fixed atoms in idealized positions (C-H = 0.98 Å). Neutral-atom scattering factors from ref 15 were used for the non-hydrogen atoms and those of ref 16 for the hydrogen atoms. Anomalous scattering factors from ref 17 were used for Hf, Zr, Cl, P, and Si atoms. In the case of the Zr complex, the absolute configuration (for the particular crystal used) has been determined through the parallel refinement of the two enantiomorphous structures that are represented by the coordinates in Table II yielding lower residuals (*R* and *R_w* ratios 1.021 and 1.022, respectively). For the monoclinic Hf complex, an isotropic type I extinction correction (Thornley–Nelmes definition of mosaic anisotropy, Lorentzian distribution) was applied^{20–22}

- (11) (a) The monoclinic form was obtained by recrystallization from toluene-hexanes as described in the Experimental Section. The orthorhombic form was obtained fortuitously from the recrystallization of Hf(CH₃)₂Cl[N(SiMe₂CH₂PM₂)₂]^{11b} by crystal picking. (b) Fryzuk, M. D.; Carter, A.; Westerhaus, A., unpublished results.
- (12) The computer programs used include locally written programs for data processing and locally modified versions of the following: ORFLS, full-matrix least squares, and ORFFE, function and errors, by W. R. Busing, K. O. Martin, and H. A. Levy; FORDAP, Patterson and Fourier syntheses, by A. Zalkin; ORTEP II, illustrations, by C. K. Johnson.
- (13) Coppens, C.; Leiserowitz, L.; Rabinovich, D., *Acta Crystallogr.* **1965**, *18*, 1035–1038.
- (14) Busing, W. R.; Levy, H. A. *Acta Crystallogr.* **1967**, *22*, 457–464.
- (15) Cromer, D. T.; Mann, J. B. *Acta Crystallogr. Sect. A: Cryst. Phys. Diffr., Theor. Gen. Crystallogr.* **1968**, *A24*, 321–324.
- (16) Stewart, R. F.; Davidson, E. R.; Simpson, W. T. *J. Chem. Phys.* **1965**, *42*, 3175–3187.
- (17) Cromer, D. T.; Liberman, D. *J. Chem. Phys.* **1970**, *53*, 1891–1898.
- (18) Schomaker, V.; Trueblood, K. N. *Acta Crystallogr., Sect. B: Struct. Crystallogr. Cryst. Chem.* **1968**, *24*, 63–76.
- (19) Cruickshank, D. W. J. *Acta Crystallogr.* **1956**, *9*, 747–756; **1956**, *9*, 754; **1961**, *14*, 896–897.
- (20) Becker, P. J.; Coppens, P. *Acta Crystallogr., Sect. A: Cryst. Phys. Diffr., Theor. Gen. Crystallogr.* **1974**, *A30*, 129; **1974**, *A30*, 148–153; **1975**, *A31*, 417–425.
- (21) Coppens, P.; Hamilton, W. C. *Acta Crystallogr., Sect. A: Cryst. Phys. Diffr., Theor. Gen. Crystallogr.* **1970**, *A26*, 71–83.

Table I. Crystallographic Data^a

compd	[(Me ₂ PCH ₂ SiMe ₂) ₂ N]HfCl ₃	[(<i>i</i> -Pr) ₂ PCH ₂ SiMe ₂) ₂ N]ZrCl ₃
formula	C ₁₀ H ₂₈ Cl ₃ HfNP ₂ Si ₂	C ₁₈ H ₄₄ Cl ₃ NP ₂ Si ₂ Zr
fw	565.31	590.25
cryst syst	monoclinic	orthorhombic
space group	<i>P</i> 2 ₁ / <i>n</i>	<i>Pbcn</i>
<i>a</i> , Å	9.6894 (10)	13.3517 (8)
<i>b</i> , Å	16.5086 (6)	20.595 (2)
<i>c</i> , Å	13.6613 (13)	15.9398 (7)
α, deg	90	90
β, deg	92.214 (4)	90
γ, deg	90	90
<i>V</i> , Å ³	2183.6 (3)	4382.9 (5)
<i>Z</i>	4	8
<i>D</i> _{calcd} , g/cm ³	1.720	1.713
<i>F</i> (000)	1104	2208
μ(Mo Kα), cm ⁻¹	53.48	53.29
cryst dimens, mm	0.16 × 0.27 × 0.41	0.28 × 0.32 × 0.38
transmissn factors	0.274–0.462	0.230–0.350
scan type	ω–2θ	ω–2θ
scan range, deg in ω	0.70 + 0.35 tan θ	0.65 + 0.35 tan θ
scan speed, deg/min	1.55–10.06	0.96–10.06
data collcd	± <i>h</i> , + <i>k</i> , + <i>l</i>	+ <i>h</i> , + <i>k</i> , + <i>l</i>
2θ _{max} , deg	60	60
no. of unique reflns	6328	6373
no. of reflns with <i>I</i> ≥ 3σ(<i>I</i>)	4305	2843
no. of variables	173	172
<i>R</i>	0.024	0.043
<i>R</i> _w	0.030	0.046
<i>S</i>	1.202	1.623
mean Δ/σ (final cycle)	0.03	0.004
max Δ/σ (final cycle)	0.18	0.03
residual density, e/Å ³	–0.48 to +0.45	–1.7 to +3.3

^a Temperature 22 °C; Enraf-Nonius CAD4-F diffractometer; Mo Kα radiation (λ_{Kα1} = 0.709 30, λ_{Kα2} = 0.713 59 Å); graphite monochromator; takeoff angle 2.7°; aperture (2.0 + tan θ) × 4.0 mm at a distance of 173 mm from the crystal; scan range extended by 25% on both sides for background measurement; σ²(*I*) = *S* + 2*B* + [0.04(*S* – *B*)]² (*S* = scan count, *B* = normalized background count); function minimized Σw(|*F*_o – |*F*_c||)² where w = 1/σ²(*F*); *R* = Σ||*F*_o – |*F*_c||/Σ|*F*_o|, *R*_w = (Σw(|*F*_o – |*F*_c||)/Σw|*F*_o|)^{1/2}; *S* = (Σw(|*F*_o – |*F*_c||)²/(*m* – *n*))^{1/2}. Values given for *R*, *R*_w, and *S* are based on those reflections with *I* ≥ 3σ(*I*).

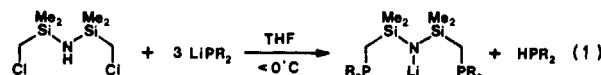
the final value of *g* being 3.85 (18) × 10⁴.

Final positional and equivalent isotropic thermal parameters are given in Table II. Anisotropic thermal parameters (Table VI), calculated hydrogen parameters (Table VII), and measured and calculated structure factor amplitudes (Tables IX–XI) are included as supplementary material.

The thermal motion in all three structures has been analyzed in terms of the rigid-body modes of translation, libration, and screw-motion.¹⁸ The rms errors in the temperature factors, σ*U*_{ij} (derived from the least-squares analyses), are 0.0024, 0.0054, and 0.0038 Å², respectively, for the monoclinic and orthorhombic Hf and the Zr complexes. The entire molecule of the monoclinic Hf complex was treated as a rigid group (rms Δ*U*_{ij} = 0.0059 Å). For the other two molecules, various structural subunits showed significant independent motion. The analyses of various 5- to 7-atom fragments gave rms Δ*U*_{ij} values in the range 0.0018–0.0054 Å². The appropriate bond lengths were corrected for libration^{18,19} with shape parameters *q*² of 0.08 for all atoms involved. Corrected and uncorrected bond lengths for the structure appear in Table III. Bond angles and intraannular torsion angles for the chelate rings are given in Tables IV and V, respectively. Complete listings of torsion angles (Table VIII) are deposited as supplementary material.

Results and Discussion

Ligand Syntheses. The addition of 1,3-bis(chloromethyl)-tetramethyldisilazane, HN(SiMe₂CH₂Cl)₂, to 3 equiv of LiPR₂ (R = Me, *i*-Pr, *t*-Bu) in tetrahydrofuran (THF) results in the direct formation of the lithium derivatives, LiN(SiMe₂CH₂PR₂)₂ (**1a**, R = Me; **1b**, R = *i*-Pr; **1c**, R = *t*-Bu), as shown in eq 1. For

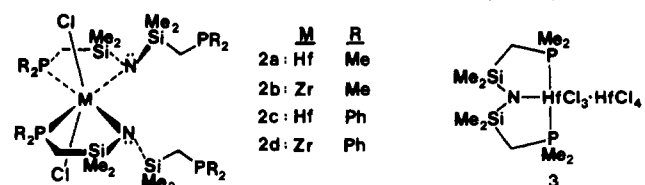


1a : R = Me
1b : R = *i*-Pr
1c : R = *t*-Bu

the analogous reaction using the less basic phosphide, LiPPh₂, only 2 equiv are used since deprotonation is not observed in this case.²³ It is noteworthy that nucleophilic displacement of the somewhat sterically hindered chlorides of HN(SiMe₂CH₂Cl)₂ proceeds smoothly even for the bulky phosphide anions to generate **1b** (R = *i*-Pr) and **1c** (R = *t*-Bu).

All of these lithium amides are colorless, air- and moisture-sensitive crystalline solids that are soluble in most organic solvents including hexanes. Purification of these ligand derivatives is normally achieved by fractional crystallization in hexanes at –30 °C, although **1a** is volatile enough to be sublimed with little decomposition.

Synthesis of MCl₃[N(SiMe₂CH₂PR₂)₂] Derivatives. The formation of bis(ligand) derivatives of the formula MCl₂[N(SiMe₂CH₂PR₂)₂]₂ (**2**) and an unusual mono(ligand) derivative of empirical formula HfCl₃[N(SiMe₂CH₂PR₂)₂]HfCl₄ (**3**) has been previously reported.^{5,6} While the former bis(ligand) derivatives, **2**, proved to be rather unreactive, the mono(ligand)hafnium



complex **3** was particularly useful in generating hydride derivatives.⁶ However, the ill-defined nature of **3** and its relative insolubility compelled us to reinvestigate the formation of mono(ligand) derivatives.

The reaction of HfCl₄ with exactly 1 equiv of sublimed **1a** in dilute toluene solutions (~0.010–~0.015 M) generates good yields

(22) Thornley, F. R.; Nelmes, R. J. *Acta Crystallogr., Sect. A: Cryst. Phys. Diffraction, Theor. Gen. Crystallogr.* 1974, *A30*, 748–757.

(23) Fryzuk, M. D.; MacNeil, P. A.; Rettig, S. J.; Secco, A. S.; Trotter, J. *Organometallics* 1982, *1*, 918–935.

(24) Clark, E. P. *Ind. Eng. Chem., Anal. Ed.* 1941, *13*, 820–822.

Table II. Final Positional (Fractional, $\times 10^5$; N and C, $\times 10^4$) and Isotropic Thermal Parameters ($10^3 U$, \AA^2) with Estimated Standard Deviations in Parentheses

atom	<i>x</i>	<i>y</i>	<i>z</i>	U_{eq}^a
Monoclinic [(Me ₂ PCH ₂ SiMe ₂) ₂ N] HfCl ₃				
Hf	43842 (2)	28358 (1)	30087 (1)	35
Cl(1)	46986 (16)	31510 (10)	47326 (9)	66
Cl(2)	57173 (15)	16044 (8)	31337 (11)	66
Cl(3)	21421 (14)	21645 (8)	30051 (12)	63
P(1)	43260 (13)	24564 (7)	10764 (8)	43
P(2)	27726 (12)	41874 (7)	30352 (10)	45
Si(1)	69835 (12)	33282 (8)	16140 (10)	44
Si(2)	56851 (13)	47153 (7)	26989 (9)	40
N	5706 (3)	3686 (2)	2389 (2)	35
C(1)	6156 (5)	2499 (4)	844 (4)	55
C(2)	4072 (5)	4920 (3)	3397 (4)	53
C(3)	3677 (7)	1484 (4)	654 (5)	76
C(4)	3507 (7)	3166 (4)	215 (4)	76
C(5)	1427 (6)	4193 (3)	3929 (5)	67
C(6)	1938 (6)	4592 (4)	1936 (5)	73
C(7)	8499 (6)	2917 (4)	2335 (5)	76
C(8)	7669 (6)	4079 (4)	735 (5)	72
C(9)	7220 (6)	5003 (4)	3482 (5)	69
C(10)	5575 (6)	5417 (3)	1634 (5)	68
Orthorhombic [(Me ₂ PCH ₂ SiMe ₂) ₂ N] HfCl ₃				
Hf	29769 (3)	39910 (2)	48598 (2)	37
Cl(1)	47794 (18)	38544 (14)	45959 (18)	69
Cl(2)	32267 (20)	34479 (18)	62023 (18)	82
Cl(3)	26059 (34)	50590 (17)	54655 (27)	113
P(1)	10283 (18)	37562 (12)	52969 (15)	43
P(2)	31924 (20)	47537 (13)	34861 (17)	53
Si(1)	17814 (18)	26512 (12)	42542 (17)	42
Si(2)	27462 (19)	34036 (14)	28791 (16)	47
N	2405 (5)	3359 (3)	3936 (4)	37
C(1)	983 (7)	2877 (4)	5191 (6)	53
C(2)	3526 (7)	4159 (5)	2704 (6)	55
C(3)	506 (8)	3939 (6)	6316 (7)	73
C(4)	90 (7)	4054 (4)	4541 (7)	65
C(5)	4141 (10)	5386 (6)	3457 (8)	93
C(6)	2079 (10)	5159 (7)	3092 (9)	100
C(7)	939 (7)	2296 (5)	3446 (7)	62
C(8)	2687 (9)	2012 (5)	4602 (8)	75
C(9)	1656 (9)	3470 (7)	2151 (7)	84
C(10)	3518 (9)	2708 (6)	2541 (8)	94
[(<i>i</i> -Pr) ₂ PCH ₂ SiMe ₂) ₂ N] ZrCl ₃				
Zr	54243 (4)	53754 (2)	64265 (2)	39
Cl(1)	40149 (18)	64530 (9)	69219 (9)	86
Cl(2)	43113 (14)	55962 (8)	51866 (7)	69
Cl(3)	66808 (14)	54536 (9)	76324 (7)	70
P(1)	37507 (13)	42791 (7)	71340 (7)	44
P(2)	76244 (12)	59812 (6)	56513 (7)	44
Si(1)	64489 (15)	35022 (8)	67020 (8)	53
Si(2)	71660 (15)	42587 (7)	51877 (7)	51
N	6362 (4)	4322 (2)	6089 (2)	41
C(1)	5042 (5)	3586 (3)	7426 (3)	60
C(2)	7632 (5)	5279 (3)	4861 (2)	52
C(3)	2482 (7)	3759 (4)	6522 (3)	76
C(4)	2770 (5)	4503 (3)	8021 (3)	56
C(5)	9235 (4)	5849 (3)	6179 (3)	51
C(6)	7704 (6)	6982 (3)	5232 (3)	63
C(7)	8022 (7)	3469 (4)	7269 (4)	86
C(8)	6271 (7)	2543 (3)	6180 (4)	81
C(9)	8790 (7)	3705 (3)	5233 (4)	85
C(10)	6078 (7)	3813 (3)	4435 (3)	74
C(11)	2928 (8)	3620 (5)	5717 (4)	104
C(12)	1977 (8)	3015 (4)	6894 (4)	102
C(13)	3621 (6)	4910 (4)	8621 (3)	77
C(14)	1527 (6)	4982 (4)	7847 (4)	87
C(15)	10457 (6)	5775 (4)	5666 (4)	77
C(16)	9432 (6)	6496 (3)	6778 (3)	68
C(17)	7260 (10)	7042 (4)	4428 (4)	114
C(18)	6977 (7)	7565 (3)	5759 (4)	81

^a $U_{eq} = 1/3[\text{trace } U_{diag}]$.**Table III.** Bond Lengths (\AA) with Estimated Standard Deviations in Parentheses

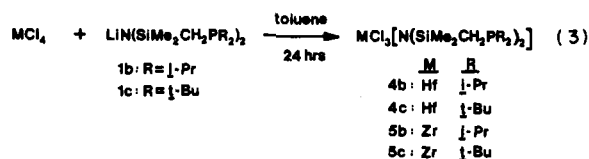
bond	uncor	cor	bond	uncor	cor
Monoclinic [(Me ₂ PCH ₂ SiMe ₂) ₂ N] HfCl ₃					
Hf-Cl(1)	2.4196 (12)	2.427	P(2)-C(5)	1.821 (5)	1.821
Hf-Cl(2)	2.4110 (12)	2.417	P(2)-C(6)	1.805 (6)	1.808
Hf-Cl(3)	2.4386 (12)	2.445	Si(1)-N	1.761 (3)	1.767
Hf-P(1)	2.7115 (11)	2.721	Si(1)-C(1)	1.887 (5)	1.892
Hf-P(2)	2.7246 (12)	2.734	Si(1)-C(7)	1.864 (6)	1.866
Hf-N	2.100 (3)	2.107	Si(1)-C(8)	1.866 (6)	1.868
P(1)-C(1)	1.815 (5)	1.821	Si(2)-N	1.752 (3)	1.758
P(1)-C(3)	1.810 (5)	1.813	Si(2)-C(2)	1.893 (5)	1.899
P(1)-C(4)	1.820 (6)	1.824	Si(2)-C(9)	1.860 (5)	1.861
P(2)-C(2)	1.801 (5)	1.806	Si(2)-C(10)	1.860 (6)	1.863
Orthorhombic [(Me ₂ PCH ₂ SiMe ₂) ₂ N] HfCl ₃					
Hf-Cl(1)	2.459 (2)	2.469	P(2)-C(5)	1.813 (11)	1.825
Hf-Cl(2)	2.435 (3)	2.447	P(2)-C(6)	1.815 (12)	1.829
Hf-Cl(3)	2.443 (3)	2.459	Si(1)-N	1.748 (7)	1.755
Hf-P(1)	2.736 (2)	2.746	Si(1)-C(1)	1.892 (10)	1.900
Hf-P(2)	2.706 (3)	2.719	Si(1)-C(7)	1.859 (10)	1.869
Hf-N	2.104 (7)	2.117	Si(1)-C(8)	1.868 (10)	1.878
P(1)-C(1)	1.811 (9)	1.820	Si(2)-N	1.748 (7)	1.758
P(1)-C(3)	1.807 (10)	1.814	Si(2)-C(2)	1.886 (9)	1.893
P(1)-C(4)	1.842 (11)	1.853	Si(2)-C(9)	1.868 (11)	1.879
P(2)-C(2)	1.799 (10)	1.812	Si(2)-C(10)	1.839 (12)	1.851
[(<i>i</i> -Pr) ₂ PCH ₂ SiMe ₂) ₂ N] ZrCl ₃					
Zr-Cl(1)	2.4627 (14)	2.472	Si(1)-C(7)	1.846 (7)	1.856
Zr-Cl(2)	2.4359 (13)	2.446	Si(1)-C(8)	1.874 (6)	1.882
Zr-Cl(3)	2.4290 (12)	2.440	Si(2)-N	1.751 (4)	1.756
Zr-P(1)	2.7833 (12)	2.789	Si(2)-C(2)	1.886 (5)	1.890
Zr-P(2)	2.7645 (12)	2.772	Si(2)-C(9)	1.872 (6)	1.880
Zr-N	2.104 (3)	2.114	Si(2)-C(10)	1.853 (6)	1.860
P(1)-C(1)	1.817 (5)	1.824	C(3)-C(11)	1.475 (9)	1.481
P(1)-C(3)	1.869 (6)	1.878	C(3)-C(12)	1.506 (9)	1.515
P(1)-C(4)	1.853 (5)	1.860	C(4)-C(13)	1.505 (8)	1.510
P(2)-C(2)	1.812 (4)	1.816	C(4)-C(14)	1.512 (8)	1.521
P(2)-C(5)	1.856 (5)	1.862	C(5)-C(15)	1.509 (7)	1.519
P(2)-C(6)	1.854 (5)	1.859	C(5)-C(16)	1.522 (7)	1.530
Si(1)-N	1.753 (4)	1.760	C(6)-C(17)	1.457 (8)	1.463
Si(1)-C(1)	1.881 (5)	1.887	C(6)-C(18)	1.527 (8)	1.534

of HfCl₃[N(SiMe₂CH₂PMe₂)₂] (**4a**) if long reaction times (≥ 5 days) are used (eq 2). The use of more concentrated solutions



generates oily mixtures of products and/or poor yields of **4a**. In solution, **4a** is monomeric (CH₂Cl₂, Signer method²⁴) and is very soluble in most organic solvents but insoluble in hydrocarbons such as hexanes. The analogous reaction of ZrCl₄ and **1a** proceeds smoothly to produce **5a**, also in very good yield (eq 2). Monitoring this reaction (eq 2, M = Hf) by ³¹P NMR shows that the bis-(ligand) derivative **2a** is the first product formed in a relatively fast step (over a few hours), followed by a slower conproportionation reaction (over a few days) with the HfCl₄ present to generate the mono(product) **4a**. Undoubtedly, the dangling phosphine arms of **2** interact with the starting MCl₄ to facilitate ligand transfer.

The use of the bulkier ligand precursors **1b** (R = *i*-Pr) and **1c** (R = *t*-Bu) in a metathesis reaction with either HfCl₄ or ZrCl₄ proceeds directly to the mono(ligand) derivatives as shown in eq 3. Notably there is no requirement for high dilution as is the



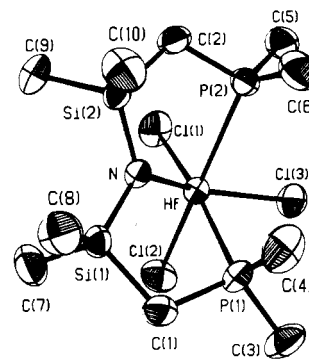
case for **1a**, and relatively short reaction times (~ 1 day) suffice for good yields of **4** and **5** (R = *i*-Pr, *t*-Bu). We have no evidence

Table IV. Bond Angles (deg) with Estimated Standard Deviations in Parentheses

Monoclinic [(Me ₂ PCH ₂ SiMe ₂) ₂ N] HfCl ₃			
Cl(1)-Hf-Cl(2)	93.75 (5)	Hf-P(2)-C(5)	116.0 (2)
Cl(1)-Hf-Cl(3)	100.27 (5)	Hf-P(2)-C(6)	122.0 (2)
Cl(1)-Hf-P(1)	173.91 (4)	C(2)-P(2)-C(5)	108.9 (3)
Cl(1)-Hf-P(2)	82.05 (5)	C(2)-P(2)-C(6)	105.4 (3)
Cl(1)-Hf-N	101.12 (10)	C(5)-P(2)-C(6)	104.3 (3)
Cl(2)-Hf-Cl(3)	95.27 (5)	N-Si(1)-C(1)	106.6 (2)
Cl(2)-Hf-P(1)	82.25 (5)	N-Si(1)-C(7)	111.2 (3)
Cl(2)-Hf-P(2)	174.47 (4)	N-Si(1)-C(8)	116.1 (2)
Cl(2)-Hf-N	104.98 (9)	C(1)-Si(1)-C(7)	109.8 (3)
Cl(3)-Hf-P(1)	84.72 (4)	C(1)-Si(1)-C(8)	106.1 (3)
Cl(3)-Hf-P(2)	82.02 (4)	C(7)-Si(1)-C(8)	106.8 (3)
Cl(3)-Hf-N	149.32 (10)	N-Si(2)-C(2)	108.2 (2)
P(1)-Hf-P(2)	102.22 (4)	N-Si(2)-C(9)	111.7 (2)
P(1)-Hf-N	75.63 (9)	N-Si(2)-C(10)	114.6 (2)
P(2)-Hf-N	79.46 (9)	C(2)-Si(2)-C(9)	108.8 (3)
Hf-P(1)-C(1)	100.2 (2)	C(2)-Si(2)-C(10)	105.0 (2)
Hf-P(1)-C(3)	120.6 (2)	C(9)-Si(2)-C(10)	108.2 (3)
Hf-P(1)-C(4)	118.2 (2)	Hf-N-Si(1)	118.2 (2)
C(1)-P(1)-C(3)	107.9 (3)	Hf-N-Si(2)	122.5 (2)
C(1)-P(1)-C(4)	105.5 (3)	Si(1)-N-Si(2)	119.0 (2)
C(3)-P(1)-C(4)	103.1 (3)	P(1)-C(1)-Si(1)	109.1 (2)
Hf-P(2)-C(2)	99.1 (2)	P(2)-C(2)-Si(2)	108.9 (2)
Orthorhombic [(Me ₂ PCH ₂ SiMe ₂) ₂ N] HfCl ₃			
Cl(1)-Hf-Cl(2)	87.96 (9)	Hf-P(2)-C(5)	120.6 (4)
Cl(1)-Hf-Cl(3)	111.60 (12)	Hf-P(2)-C(6)	117.2 (4)
Cl(1)-Hf-P(1)	162.59 (9)	C(2)-P(2)-C(5)	107.1 (5)
Cl(1)-Hf-P(2)	79.82 (9)	C(2)-P(2)-C(6)	105.8 (6)
Cl(1)-Hf-N	99.5 (2)	C(5)-P(2)-C(6)	103.7 (7)
Cl(2)-Hf-Cl(3)	95.16 (14)	N-Si(1)-C(1)	107.1 (4)
Cl(2)-Hf-P(1)	79.98 (8)	N-Si(1)-C(7)	114.4 (4)
Cl(2)-Hf-P(2)	163.89 (10)	N-Si(1)-C(8)	111.1 (4)
Cl(2)-Hf-N	112.5 (2)	C(1)-Si(1)-C(7)	107.6 (5)
Cl(3)-Hf-P(1)	82.19 (11)	C(1)-Si(1)-C(8)	107.6 (5)
Cl(3)-Hf-P(2)	79.85 (12)	C(7)-Si(1)-C(8)	108.8 (5)
Cl(3)-Hf-N	138.9 (2)	N-Si(2)-C(2)	109.2 (4)
P(1)-Hf-P(2)	114.13 (8)	N-Si(2)-C(9)	113.6 (4)
P(1)-Hf-N	74.0 (2)	N-Si(2)-C(10)	112.9 (5)
P(2)-Hf-N	80.1 (2)	C(2)-Si(2)-C(9)	106.2 (5)
Hf-P(1)-C(1)	100.5 (3)	C(2)-Si(2)-C(10)	106.5 (5)
Hf-P(1)-C(3)	124.0 (4)	C(9)-Si(2)-C(10)	108.2 (6)
Hf-P(1)-C(4)	114.9 (3)	Hf-N-Si(1)	118.8 (4)
C(1)-P(1)-C(3)	106.1 (5)	Hf-N-Si(2)	123.2 (3)
C(1)-P(1)-C(4)	104.2 (5)	Si(1)-N-Si(2)	116.5 (4)
C(3)-P(1)-C(4)	104.9 (5)	P(1)-C(1)-Si(1)	107.4 (4)
Hf-P(2)-C(2)	101.3 (3)	P(2)-C(2)-Si(2)	108.5 (4)
[(i-Pr) ₂ PCH ₂ SiMe ₂) ₂ N] ZrCl ₃			
Cl(1)-Zr-Cl(2)	85.99 (5)	N-Si(1)-C(7)	112.6 (3)
Cl(1)-Zr-Cl(3)	87.46 (6)	N-Si(1)-C(8)	113.6 (2)
Cl(1)-Zr-P(1)	90.42 (5)	C(1)-Si(1)-C(7)	106.4 (3)
Cl(1)-Zr-P(2)	109.90 (5)	C(1)-Si(1)-C(8)	108.3 (3)
Cl(1)-Zr-N	169.68 (11)	C(7)-Si(1)-C(8)	107.9 (3)
Cl(2)-Zr-Cl(3)	167.44 (5)	N-Si(2)-C(2)	108.7 (2)
Cl(2)-Zr-P(1)	102.46 (4)	N-Si(2)-C(9)	112.9 (2)
Cl(2)-Zr-P(2)	83.03 (4)	N-Si(2)-C(10)	112.3 (2)
Cl(2)-Zr-N	95.20 (10)	C(2)-Si(2)-C(9)	105.3 (3)
Cl(3)-Zr-P(1)	88.28 (4)	C(2)-Si(2)-C(10)	108.2 (2)
Cl(3)-Zr-P(2)	89.16 (4)	C(9)-Si(2)-C(10)	109.1 (3)
Cl(3)-Zr-N	93.16 (10)	Zr-N-Si(1)	122.3 (2)
P(1)-Zr-P(2)	159.38 (4)	Zr-N-Si(2)	120.1 (2)
P(1)-Zr-N	79.30 (10)	Si(1)-N-Si(2)	117.6 (2)
P(2)-Zr-N	80.42 (10)	P(1)-C(1)-Si(1)	113.0 (3)
Zr-P(1)-C(1)	97.7 (2)	P(2)-C(2)-Si(2)	112.5 (2)
Zr-P(1)-C(3)	118.4 (2)	P(1)-C(3)-C(11)	113.8 (5)
Zr-P(1)-C(4)	122.6 (2)	P(1)-C(3)-C(12)	112.6 (5)
C(1)-P(1)-C(3)	109.0 (3)	C(11)-C(3)-C(12)	111.5 (6)
C(1)-P(1)-C(4)	106.1 (2)	P(1)-C(4)-C(13)	111.4 (3)
C(3)-P(1)-C(4)	102.0 (3)	P(1)-C(4)-C(14)	112.3 (4)
Zr-P(2)-C(2)	96.9 (2)	C(13)-C(4)-C(14)	110.3 (5)
Zr-P(2)-C(5)	113.68 (15)	P(2)-C(5)-C(15)	114.8 (4)
Zr-P(2)-C(6)	124.4 (2)	P(2)-C(5)-C(16)	110.9 (3)
C(2)-P(2)-C(5)	106.5 (2)	C(15)-C(5)-C(16)	110.7 (4)
C(2)-P(2)-C(6)	108.3 (2)	P(2)-C(6)-C(17)	115.0 (5)
C(5)-P(2)-C(6)	105.4 (2)	P(2)-C(6)-C(18)	110.2 (4)
N-Si(1)-C(1)	107.6 (2)	C(17)-C(6)-C(18)	112.1 (5)

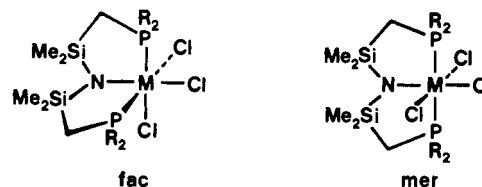
Table V. Intraannular Torsion Angles (deg) with Standard Deviations in Parentheses

Monoclinic [(Me ₂ PCH ₂ SiMe ₂) ₂ N] HfCl ₃			
N-Hf-P(1)-C(1)	45.6 (2)	N-Hf-P(2)-C(2)	-40.4 (2)
Hf-P(1)-C(1)-Si(1)	-35.1 (3)	Hf-P(2)-C(2)-Si(2)	42.5 (3)
N-Si(1)-C(1)-P(1)	6.6 (4)	N-Si(2)-C(2)-P(2)	-26.5 (3)
C(1)-Si(1)-N-Hf	40.0 (3)	C(2)-Si(2)-N-Hf	-13.0 (3)
P(1)-Hf-N-Si(1)	-49.3 (2)	P(2)-Hf-N-Si(2)	30.9 (2)
Orthorhombic [(Me ₂ PCH ₂ SiMe ₂) ₂ N] HfCl ₃			
N-Hf-P(1)-C(1)	47.4 (4)	N-Hf-P(2)-C(2)	-36.4 (4)
Hf-P(1)-C(1)-Si(1)	-37.1 (5)	Hf-P(2)-C(2)-Si(2)	39.8 (5)
N-Si(1)-C(1)-P(1)	8.4 (6)	N-Si(2)-C(2)-P(2)	-26.5 (6)
C(1)-Si(1)-N-Hf	40.3 (5)	C(2)-Si(2)-N-Hf	-8.1 (6)
P(1)-Hf-N-Si(1)	-50.2 (3)	P(2)-Hf-N-Si(2)	25.6 (4)
[(i-Pr) ₂ PCH ₂ SiMe ₂) ₂ N] ZrCl ₃			
N-Zr-P(1)-C(1)	38.1 (2)	N-Zr-P(2)-C(2)	39.8 (2)
Zr-P(1)-C(1)-Si(1)	-36.0 (3)	Zr-P(2)-C(2)-Si(2)	-37.3 (3)
N-Si(1)-C(1)-P(1)	17.0 (4)	N-Si(2)-C(2)-P(2)	18.0 (3)
C(1)-Si(1)-N-Zr	23.3 (3)	C(2)-Si(2)-N-Zr	23.0 (3)
P(1)-Zr-N-Si(1)	-36.3 (2)	P(2)-Zr-N-Si(2)	-36.7 (2)

Figure 1. Structure and numbering scheme of the monoclinic form of HfCl₃[N(SiMe₂CH₂PMe₂)₂] (**4a**).

to support the intermediacy of the bis(ligand) derivatives for R = *i*-Pr and *t*-Bu.

Solution and Solid-State Structures of MCl₃[N(SiMe₂CH₂PR₂)₂] Derivatives. Having established that these mono(ligand) derivatives were monomeric, our attention turned to the determination of the stereochemistry of these species. The ³¹P{¹H} NMR spectra indicated that these ligands were bound in a tridentate coordination mode since the chemically equivalent phosphorus donors resonated at, typically, lower field than the free, uncoordinated nuclei. On the basis of an octahedral geometry, two limiting stereochemistries for these MCl₃[N(SiMe₂CH₂PR₂)₂] derivatives are possible: facial (*fac*) or meridional (*mer*).



We were able, fortuitously,¹¹ to crystallize two distinct forms of the hafnium complex HfCl₃[N(SiMe₂CH₂PMe₂)₂], **4a** (monoclinic) and **4a'** (orthorhombic), and determine their solid-state structures. The results are shown in Figures 1 and 2, respectively. Both structures have the ligand bound in a tridentate, facial mode, but there are large deviations from pure octahedral geometry. In **4a** (Figure 1), the Cl(3)-Hf-N bond angle (Table IV) is 149.32 (10)°, or alternatively, the amide nitrogen is displaced 30.7° away from a pure trans orientation to Cl(3). In **4a'** (Figure 2), this distortion is larger; now the amide nitrogen deviates 41.1° away from the expected trans disposition. Of course, this increased distortion in **4a'** affects many of the other bond angles; for example, the P(1)-Hf-P(2) angle of 102.22 (4)° in **4a** opens up to 114.13 (8)° in **4a'**. In fact, the only angles that remain relatively constant in both **4a** and **4a'** are the P(1)-Hf-N and

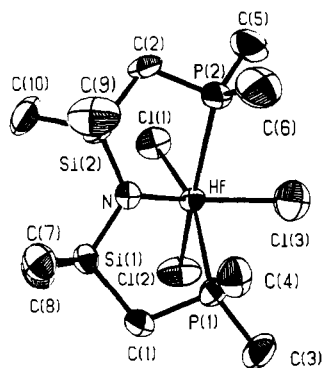


Figure 2. Structure and numbering scheme of the orthorhombic form of $\text{HfCl}_3[\text{N}(\text{SiMe}_2\text{CH}_2\text{PMe}_2)_2]$ ($4a'$).

$\text{P}(2)\text{-Hf-N}$ bite angles and the angles of the planar NSi_2 units in the ligands. The bond lengths (Table III) are also slightly different between $4a$ and $4a'$, but not markedly so. The corrected Hf-Cl bond lengths range from 2.417 to 2.469 Å, while the Hf-P bond lengths range from 2.719 to 2.746 Å; the Hf-N bond length of 2.107 Å in $4a$ is very similar to the 2.117 Å distance found in $4a'$.

When crystals of $4a$ or $4a'$ are dissolved in benzene or dichloromethane, their solution spectroscopic properties (^1H and $^{13}\text{C}\{^1\text{H}\}$ NMR) are consistent with an isomerization to the meridional geometry (eq 4). Thus, the ^1H NMR shows only one

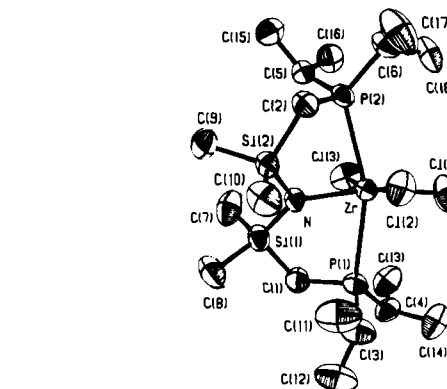
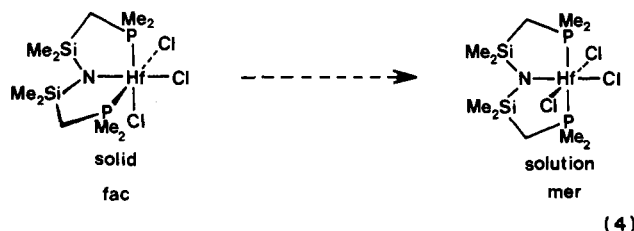


Figure 3. Structure and numbering scheme for $\text{mer-ZrCl}_3[\text{N}(\text{SiMe}_2\text{CH}_2\text{P}(i\text{-Pr})_2)_2]$ ($5b$).

type of environment for each of the different protons on the ligand as expected for a molecule with C_{2v} symmetry; a static facial geometry (C_3 symmetry) would have two different types of silyl methyl (SiCH_3) and phosphorus methyl (PCH_3) environments as well as an AA'BB'XX' spin system (where X and X' are the ^{31}P nuclei) for the methylene (PCH_2Si) protons. The fact that the $^{13}\text{C}\{^1\text{H}\}$ NMR also shows only one silyl methyl environment, even down to -90°C , tends to rule out fluxional processes involving facial geometries.²⁵

In a meridional geometry, the methylene protons can be described as an $\text{A}_2\text{A}_2'\text{XX}'$ spin system, which in certain situations reduces²⁶ to an A_4X_2 virtual triplet with strong phosphorus-phosphorus coupling ($^2J_{\text{XX}'}$ is large). Assigning stereochemistry using the shape of this pattern is fraught with uncertainty,²⁷ as is true in our case since we observe a filled-in doublet pattern (vide infra) for these resonances rather than a virtual triplet as might be predicted from trans-disposed phosphorus donors. The zirconium analogue $5a$ shows nearly identical spectroscopic parameters.

We were interested in examining the effect of bulky substituents on the phosphorus donors on the solution and solid-state stereochemistries. The single-crystal X-ray structure of $\text{ZrCl}_3[\text{N}(\text{SiMe}_2\text{CH}_2\text{P}(i\text{-Pr})_2)_2]$ ($5b$) is shown in Figure 3. In this case, the solid-state structure shows an irregular octahedral geometry, wherein the tridentate ligand binds in a meridional fashion. The deviations from octahedral geometry are easily apparent: the $\text{P}(1)\text{-Zr-P}(2)$ angle (Table IV) is $159.38(4)^\circ$, bent back $\sim 20^\circ$ from a pure trans orientation; the remaining bond angles are also less than 180° , but only by $\sim 10\text{-}12^\circ$ (for example, the $\text{Cl}(1)\text{-}$

Figure 4. 80-MHz ^1H NMR spectrum of $\text{mer-HfCl}_3[\text{N}(\text{SiMe}_2\text{CH}_2\text{P}(i\text{-Bu})_2)_2]$.

Zr-N angle is $167.44(5)^\circ$). The Zr-P bond lengths (Table III) of 2.772 and 2.789 Å are only marginally shorter than those reported⁵ for the bis(ligand) derivative $\text{ZrCl}_2[\text{N}(\text{SiMe}_2\text{CH}_2\text{PMe}_2)_2]$ (i.e., 2.7936 (13), 2.8028 (12) Å). The Zr-N and Zr-Cl bond lengths of $5b$ are virtually the same as found in the bis(ligand) complex; the remaining bond lengths and bond angles are not unusual.

In solution, $5b$ appears to retain the meridional geometry on the basis of ^1H NMR results since, once again, only one type of SiCH_3 is observed even down to -90°C ; however, the methylene (PCH_2Si) protons and the isopropyl methyl ($\text{PCH}(\text{CH}_3)_2$) protons overlap except at high field (400 MHz). A more simple ^1H NMR spectrum is achieved with the bulkier $t\text{-Bu}$ substituents on phosphorus; thus, the ^1H NMR spectra (Figure 4) of $\text{MCl}_3[\text{N}(\text{SiMe}_2\text{CH}_2\text{P}(t\text{-Bu})_2)_2]$ ($M = \text{Hf}$, $4c$; $M = \text{Zr}$, $5c$) are remarkably similar to that described above for the $-\text{PMe}_2$ derivatives $4a$ and $5a$. For $4c$ and $5c$, filled-in doublets for both the *tert*-butyl ($\text{PC}(\text{CH}_3)_3$) and methylene (PCH_2Si) protons are observed, as well as a sharp singlet for the silyl methyl (SiCH_3) protons, all consistent with a meridional geometry. Indeed, we are convinced that all of the mono(ligand) derivatives, $\text{MCl}_3[\text{N}(\text{SiMe}_2\text{CH}_2\text{PR}_2)_2]$ (4 and 5 ; $R = \text{Me}$, $i\text{-Pr}$, $t\text{-Bu}$; $M = \text{Zr}$, Hf), exist in solution exclusively in the meridional configuration.

The far-IR region on solid samples (CsI disks) did not provide definitive information on solid-state stereochemistry; the $M\text{-N}$

(25) We consider it unlikely that a fluxional process involving $\text{fac} \rightarrow \text{mer}$ geometry changes is occurring simply because the structural reorganization required is immense.

(26) Harris, R. K. *Can. J. Chem.* **1964**, *42*, 2275-2281.

(27) Ogilvie, F. B.; Jenkins, J. M.; Verkade, J. G. *J. Am. Chem. Soc.* **1970**, *92*, 1916-1923.

and M-Cl vibration band patterns²⁸ did not show distinct differences between known fac (**4a**) and mer (**5b**) geometries. In fact, the zirconium analogue of **4a**, $ZrCl_3[N(SiMe_2CH_2PMe_2)_2]$ (**5a**), displayed more absorptions in the far-IR region than any of the other mono(ligand) derivatives; it is possible that this zirconium complex crystallizes as a mixture of fac and mer, but this is pure speculation.

Conclusions

It would appear that these tridentate ligands prefer the meridional geometry in solution, but in the solid state other factors, presumably crystal packing, determine the coordination mode. The ligand's preference for the meridional configuration may be due to the planar M-NSi₂ unit found in all of these derivatives,^{5,6,23,29} which could be less strained when the phosphine arms are trans disposed as compared to the cis orientation in the facial mode. Alternatively, it may be that the meridional geometry is preferred simply on steric grounds since this would minimize intramolecular, nonbonding repulsions between the -PR₂ groups of the ligand; while this is tenable for the bulky R = *i*-Pr and *t*-Bu substituents, molecular models of the -PMe₂ derivatives and the X-ray crystal structures of **4a** and **4a'** do not show any obvious steric congestion in the facial bonding mode. Certainly the for-

mally d⁰ metal centers (Zr(IV), Hf(IV)) would not be expected to exert any stereochemical influence.

These mono(ligand) derivatives are very reactive and can be used to generate group 4³⁰ alkyl and hydride derivatives; full details of this will be reported in due course.

Acknowledgment. Financial support for this research was provided by the Natural Sciences and Engineering Research Council of Canada. We gratefully acknowledge both Professor James Trotter for the use of his X-ray diffractometer and structure solving programs and Dr. Steven J. Rettig of the UBC Crystal Structure Service for collecting the data and solving the structures.

Registry No. *fac-4a*, 94372-14-2; *mer-4a*, 94481-25-1; **4b**, 94372-16-4; **4c**, 94372-18-6; **5a**, 94372-15-3; **5b**, 94372-17-5; **5c**, 94372-19-7; LiN(SiMe₂CH₂PMe₂)₂, 94372-10-8; HN(SiMe₂CH₂Cl)₂, 14579-91-0; HN(SiMe₂CH₂PMe₂)₂, 94372-11-9; LiN(SiMe₂CH₂P(*i*-Pr)₂)₂, 94372-12-0; LiN(SiMe₂CH₂P(*t*-Bu)₂)₂, 94372-13-1; HP(*t*-Bu)₂, 819-19-2; LiPMe₂, 21743-25-9; LiP(*i*-Pr)₂, 21502-53-4.

Supplementary Material Available: Listings of anisotropic thermal parameters (Table VI), calculated hydrogen coordinates and isotropic thermal parameters (Table VII), torsion angles (Table VIII), and observed and calculated structure factor amplitudes (Table IX-XI) (87 pages). Ordering information is given on any current masthead page.

(30) The group notation is being changed in accord with recent actions by IUPAC and ACS nomenclature committees. A and B notation is being eliminated because of wide confusion. Group I becomes groups 1 and 11, group II becomes groups 2 and 12, group III becomes groups 3 and 13, etc.

- (28) Andersen, R. A. *Inorg. Chem.* 1979, 18, 1724-1725, 2928-2932.
 (29) Lappert, M. F.; Power, P. P.; Sanger, A. R.; Srivastava, R. C. "Metal and Metalloid Amides", Wiley: New York, 1980; p 488.

Contribution from the Istituto di Chimica Generale, Università di Pisa, 56100 Pisa, Italy, and Istituto di Strutturistica Chimica, Centro di Studio per la Strutturistica Diffraattometrica del CNR, Università di Parma, 43100 Parma, Italy

Reaction of Copper(I)-*N,N'*-Ethylenebis(benzaldimine) Complexes with Carbon Monoxide and Isocyanides

ANDRAS TOTH,[†] CARLO FLORIANI,^{*†} MARCO PASQUALI,[†] ANGIOLA CHIESI-VILLA,[‡] AMELIA GAETANI-MANFREDOTTI,[‡] and CARLO GUASTINI[†]

Received May 11, 1984

Copper(I) halides, CuX (X = Cl, I), react with *N,N'*-ethylenebis(benzaldimine), BEN (PhCH=NCH₂CH₂N=CHPh), in a 1:1 molar ratio to form final products that are probably the dimers [Cu₂X₂(BEN)₂] (II) via the intermediacy of monomeric solvated species, [Cu(X)(BEN)(S)] (I). A monomeric complex is isolated, when S = CO, by reacting CuI with BEN in a carbon monoxide atmosphere ([Cu(BEN)(CO)(I)] (III), $\nu(C-O) = 2066\text{ cm}^{-1}$). With *p*-tolyl isocyanide the analogous monomeric complex [Cu(BEN)(*p*-MeC₆H₄NC)(I)] (IV) ($\nu(C-N) = 2135\text{ cm}^{-1}$) is formed. The structures of complexes III and IV were determined by X-ray analyses, showing pseudotetrahedral coordination geometry for Cu(I) in both complexes (C-O = 1.12 (2) Å, *p*-MeC₆H₄N-C = 1.17 (1) Å). Derivative III represents the first example of a monomeric complex containing the [X-Cu-CO] fragment. When CuI is reacted with an excess of BEN under a carbon monoxide atmosphere and in the presence of NaBPh₄, ionization occurs to form [Cu(BEN)₂](BPh₄) (V). The cation [Cu(BEN)₂]⁺ possesses S₄ symmetry. In complexes II-V the C-N bond distances and stretching vibrations of ligated BEN are only slightly affected by the coordination to copper(I) and vary as follows: 1.267 (5)-1.28 (1) Å; 1625-1635 cm⁻¹. The ligated BEN does not cause a significant disproportionation of copper(I) to copper(II) and copper metal, even in the absence of carbon monoxide, while providing the appropriate electronic properties for binding CO. Such a ligand as BEN seems to affect the electronic balance at the metal by an extent that is intermediate between those of saturated amino ligands and of nitrogen donor heterocycles such as pyridine and 2,2'-bipyridine. Carbonylation of [Cu(PhCO₂)₂]₄, carried out in the presence of BEN, allows the isolation in the solid state of a dicopper(I) complex containing a bridging carbonyl ($\nu(C-O) = 1958\text{ cm}^{-1}$ (Nujol)), [Cu₂(PhCO₂)₂(BEN)(μ -CO)] (X). Crystallographic details for complexes III-V are as follows: complex III, space group P2₁/n (monoclinic), *a* = 7.113 (2) Å, *b* = 17.204 (4) Å, *c* = 14.794 (4) Å, $\beta = 97.87$ (3)°, *Z* = 4, *D*_{calcd} = 1.68 g cm⁻³, *V* = 1793.3 (8) Å³, final *R* factor 0.043 for 1698 observed reflections; complex IV, space group P1̄ (triclinic), *a* = 10.139 (7) Å, *b* = 13.427 (6) Å, *c* = 9.830 (4) Å, $\alpha = 91.56$ (5)°, $\beta = 111.31$ (5)°, $\gamma = 108.54$ (5)°, *Z* = 2, *D*_{calcd} = 1.55 g cm⁻³, *V* = 1167 (1) Å³, *R* factor 0.042 for 2464 observed reflections; complex V, space group I4₁/a (tetragonal), *a* = 17.167 (2) Å, *b* = 17.167 (2) Å, *c* = 15.463 (1) Å, *Z* = 4, *D*_{calcd} = 1.24 g cm⁻³, *V* = 4557.0 (9) Å³, final *R* factor 0.040 for 1049 observed reflections.

Introduction

A significant objective in copper(I) chemistry is the synthesis of a complex having a vacant coordination site and electron availability on the metal. These properties are a general prerequisite for the coordination and activation of small molecules like

carbon monoxide or dioxygen. Many ligands stabilize the +1 oxidation state for copper, but only a few impart the appropriate properties for reaction with small molecules. Molecules containing S and P donor atoms are ligands par excellence for copper(I),¹

[†] Università di Pisa.
[‡] Università di Parma.

(1) (a) Jardine, F. H. *Adv. Inorg. Chem. Radiochem.* 1975, 17, 115-163.
 (b) Gill, J. T.; Mayerle, J. J.; Welcker, P. S.; Lewis, D. F.; Ucko, D. A.; Barton, D. J.; Stowens, D.; Lippard, S. J. *Inorg. Chem.* 1976, 15, 1155-1168.